Component Analysis and Accuracy Improvement of Linear Power Flow Equation based on Legendre Polynomial Expansion

Zhexin Fan, Zhifang Yang, Juan Yu, and Thomas Morstyn

***Abstract*—The linearization of the power flow equation is widely used in power industry. Existing linearization approaches are generally regarded as nonlinear state variable space transformation, where the original power flow equation can be approximately reformulated as the linear forms in transformed state variable spaces. However, the optimality of linear power flow equations cannot be theoretically compared in different spaces and is only verified based on case studies. In this paper, based on Legendre polynomial expansion, power flow equations are uniformly transformed into a single state variable space, where dimensions correspond to certain orders of Legendre expansion. Through component analysis of power flow equations on each dimension, we find that the accuracy of the linear power flow equation can be improved by formulating an appropriate state variable space transformation to reduce Legendre component loss. Based on this, a linearization method minimizing Legendre component loss is formulated. Compared with the regular case-based linearization, the proposed method does not depend on empirical data, and can theoretically guide the selection of the linear power flow equation within the specified operating bound. The accuracy performance is verified in OPF calculation based on numerous IEEE and Polish test systems.**

***Index Terms*—Power flow equation, linearization method, Taylor series expansion, Legendre polynomial expansion, operating bound.**

NOMENCLATURE

Symbols:

$A_n^g, A_{ij,n}^{cos}, A_{ij,n}^{sin}$	n-order magnitude of Legendre polynomials
$A_{n_1n_2n_3}^P, A_{n_1n_2n_3}^Q$	$n_1n_2n_3$-order magnitude of ternary Legendre polynomials of branch active/reactive power flow
$\Delta A_{ij,n_1n_2n_3}^{P,k=1,2}$	Error of the magnitude of $A_{n_1n_2n_3}^P$ when $k=1,2$ on branch $\{ij\}$
P, Q	Active/reactive power
$P_{ij}^{loss}, Q_{ij}^{loss}$	Branch active/reactive power loss from i to j
P_{ij}^f, Q_{ij}^f	Branch active/reactive power in transformed state variable space
$T_n(x)$	n-order Legendre polynomial
V_i, Φ_{ij}	Normalized voltage magnitude and angle
g_{ij}, b_{ij}, x_{ij}	Conductance/Susceptance/Inductance on branch $\{ij\}$
v, θ	Voltage magnitude and angle, state variables
$\Delta v, \Delta\theta$	Maximum variation of state variables
$\varphi_i(v_i), \phi_{ij}(\theta_{ij})$	General function form of transformed state variables
$\varphi_i'(v_i), \phi_{ij}'(\theta_{ij})$	Derivative of $\varphi_i(v_i), \phi_{ij}(\theta_{ij})$

Vector/Matrix:

$\mathbf{f}_{ij}, \mathbf{f}_{ij,0}$	(Initial) functional state variables
$\mathbf{x}_{ij}$	Vector of state variables
$\mathbf{x}_{ij}^{norm}$	Normalized vector of state variables

Index/Sets/Number:

i, j	Bus indexes
n, n_l, m	Order indexes of Legendre polynomials,$l=1,2,3$
$\mathcal{J}$	Bus set
$\mathcal{B}$	Branch set, $\mathcal{B}=\mathcal{J}\times\mathcal{J}$
$\mathcal{N}$	Set of component index of Legendre polynomials

Symbol Derivation Rule: Bold symbols represent vectors of corresponding symbols. The symbol "$\rightarrow$" represents the transformation flow. The superscript "L" represents the linear approximation of the corresponding function. The symbol "f'" represents the derivative of f.

I. INTRODUCTION

A. Research Motivation

POWER flow equation is the basic law that determines the power flow distribution in the power system [1]. It is modeled as the nonlinear projection from state variable $\mathbf{x}_{ij} = (v_i, v_j, \theta_{ij})^T$ to branch power flow (P_{ij}, Q_{ij}) [2], as shown in

$$P_{ij}(\mathbf{x}_{ij}) = g_{ij}v_i^2 - v_iv_j(g_{ij}\cos\theta_{ij} + b_{ij}\sin\theta_{ij}), \quad (1)$$

$$Q_{ij}(\mathbf{x}_{ij}) = -b_{ij}v_i^2 + v_iv_j(b_{ij}\cos\theta_{ij} - g_{ij}\sin\theta_{ij}). \quad (2)$$

The nonlinearity of the power flow equation makes power dispatching is a nonconvex optimization problem, where the global optimal solution cannot be guaranteed in finite time, i.e., non-deterministic polynomial-time (NP) hard [3], [4]. Considering the development of commercial linear programming (LP) solvers, the linear approximation of the power flow equation is widely used to satisfy the demand of computational efficiency in the power industry [5]. With the increasing stochasticity and flexibility in modern power system, such as renewable energy

This work was supported by the National Natural Science Foundation of China under Grant 52177072. *(Corresponding author: Zhifang Yang.)*

Zhexin Fan, Zhifang Yang and Juan Yu are with the State Key Laboratory of Power Transmission Equipment & System Security and New Technology, College of Electrical Engineering, Chongqing University, Chongqing 400044, China. Thomas Morstyn is with the School of Engineering, University of Edinburgh, Edinburgh EH9 3JL, U.K. (e-mail: zfyang@cqu.edu.cn).

[6], [7], flexible transmission [8], [9], and demand response [10], [11], the improvement of linear power flow equations will bring potential economic benefits [12].

Existing linearization approaches generally employ empirical operating data to ensure the accuracy. The basic idea of the general linear power flow model is 1) to regard power flow equations (1)-(2) as the function of (P_{ij}, Q_{ij}) with respect to general function form $\mathbf{f}_{ij} = (\varphi_i(v_i), \varphi_j(v_j), \theta_{ij})$, denoted as $(P_{ij}^f(\mathbf{f}_{ij}), Q_{ij}^f(\mathbf{f}_{ij}))$ and 2) to derive the first-order Taylor expansion of $P_{ij}^f(\mathbf{f}_{ij}), Q_{ij}^f(\mathbf{f}_{ij})$ at the empirical operating point $\mathbf{f}_{ij,0} = (\varphi_i(v_{i,0}), \varphi_j(v_{j,0}), \phi_{ij}(\theta_{ij,0}))^T$ [13], as shown in

$$\begin{aligned} &P_{ij}(\mathbf{x}_{ij}) = P_{ij}({\mathbf{f}_{ij}}^{-1}(\mathbf{f}_{ij}(\mathbf{x}_{ij}))) = P_{ij}^f(\mathbf{f}_{ij}) \\ &\approx P_{ij}^f(\mathbf{f}_{ij,0}) + (\mathbf{f}_{ij} - \mathbf{f}_{ij,0})^T \nabla P_{ij}^f(\mathbf{f}_{ij,0}) \overset{define}{=} P_{ij}^L(\mathbf{f}_{ij}), \end{aligned} \tag{3}$$

$$\begin{aligned} &Q_{ij}(\mathbf{x}_{ij}) = Q_{ij}({\mathbf{f}_{ij}}^{-1}(\mathbf{f}_{ij}(\mathbf{x}_{ij}))) = Q_{ij}^f(\mathbf{f}_{ij}) \\ &\approx Q_{ij}^f(\mathbf{f}_{ij,0}) + (\mathbf{f}_{ij} - \mathbf{f}_{ij,0})^T \nabla Q_{ij}^f(\mathbf{f}_{ij,0}) \overset{define}{=} Q_{ij}^L(\mathbf{f}_{ij}), \end{aligned} \tag{4}$$

where transformation "$P_{ij}(\mathbf{x}_{ij}) \rightarrow P_{ij}^f(\mathbf{f}_{ij}) \rightarrow P_{ij}^L(\mathbf{f}_{ij})$" and "$Q_{ij}(\mathbf{x}_{ij}) \rightarrow Q_{ij}^f(\mathbf{f}_{ij}) \rightarrow Q_{ij}^L(\mathbf{f}_{ij})$" represent that the original power flow equation is transformed from state variable space $(\mathbf{x}_{ij}, P_{ij}, Q_{ij})$ to state variable space $(\mathbf{f}_{ij}, P_{ij}, Q_{ij})$ (The two space is denoted as in $\mathbf{x}_{ij}$-space and $\mathbf{f}_{ij}$-space in the following part). It is worth noting that the nonlinearity transfers from the power flow equation to state variable space transformation "$\mathbf{x}_{ij} \rightarrow \mathbf{f}_{ij}$", which is defined by $\mathbf{f}_{ij} = (\varphi_i(v_i), \varphi_j(v_j), \phi_{ij}(\theta_{ij}))^T$. The specific formulation of $\mathbf{f}_{ij}$ corresponds to a certain linear power flow equation. The commonly-used linear power flow equations are reviewed in section I-B.

However, the performance of these empirical-data-based approaches is not stable under accidental operating states of the power system [14]. Also, the optimality of linear power flow equations in different state variable spaces cannot be theoretically proven. The linearization error is generally compared based on case studies [15]. In fact, the dispatch accuracy in the power system with wide operating bound is guaranteed by iterative modifying the formulation of the linear power equation, where the frequently remodeling might cost more computational resources than the solving stage [16]. Hence, there is an urgent need to propose a high-accuracy linear power flow equation within the entire operating bound.

To tackle this issue, we uniformly transform power flow equations into a single state variable space based on Legendre polynomial expansion within the specific operation bound of the power system. Through component analysis in each dimension of the state variable space, power flow equations are theoretically compared without empirical data. In addition, a linear power flow equation minimizing the component loss within the specified operating bound is formulated. The performance is verified in OPF calculation based on numerous IEEE and Polish test systems.

B. Literature Review

The specifical linear power flow equation corresponds to the linear power flow equation (3)-(4) with the certain form of $\mathbf{f}_{ij}$. The commonly used methods are reviewed as follows.

1) DC power flow equation with $\mathbf{f}_{ij} = (v_i^0, v_j^0, \theta_{ij})$: It is based on the empirical knowledge that the ratio of r_{ij}/x_{ij} is approximately 0 and the power system operates around the initial point $(v_{i,0} = v_{j,0} = 1\ p.u., \theta_{ij} = 0)$, as shown in

$$P_{ij} = \frac{\theta_{ij}}{x_{ij}}. \tag{5}$$

This MW-only approach ignores reactive power Q and voltage magnitude v. It cannot adapt to the scenarios when Q or v are the primary concern. The derivation and application can be respectively found in [17] and [18].

2) Linear power flow equation with $\mathbf{f}_{ij} = (v_i^1, v_j^1, \theta_{ij})$: It is the basic first-order Taylor expansion of the power flow equation under the assumption that the initial point $(v_{i,0} = v_{j,0} = 1\ p.u., \theta_{ij,0} = 0)$, as shown in

$$P_{ij} = g_{ij}(v_i - v_j) - b_{ij}\theta_{ij}, \tag{6}$$

$$Q_{ij} = -b_{ij}(v_i - v_j) - g_{ij}\theta_{ij}. \tag{7}$$

The derivation and application can be respectively found in [19] and [20].

3) Linear power flow equation with $\mathbf{f}_{ij} = (v_i^2, v_j^2, \theta_{ij})$: It considers the component of voltage magnitude in the original power flow equation is quadratic [21]. Hence, the quadratic form of $\mathbf{f}_{ij} = (v_i^2, v_j^2, \theta_{ij})$ is employed to improve the accuracy. The linear power flow equation is shown as

$$P_{ij} = g_{ij}(\frac{{v_i}^2}{2} - \frac{{v_j}^2}{2}) - b_{ij}\theta_{ij}, \tag{8}$$

$$Q_{ij} = -b_{ij}(\frac{{v_i}^2}{2} - \frac{{v_j}^2}{2}) - g_{ij}\theta_{ij}. \tag{9}$$

The derivation and improvement discussion can be respectively found in [22]. In conclusion, according to (3)-(4), the detailed formulation of the commonly-used linear power flow can be unified as

$$\begin{aligned} P_{ij}^L(\mathbf{f}_{ij}) = g_{ij}[&(\varphi_i(v_i) - \varphi_i(v_{i,0}))/{\varphi'}_i(v_{i,0}) \\ &-(\varphi_j(v_j) - \varphi_j(v_{j,0}))/{\varphi'}_j(v_{j,0})] \\ &-b_{ij}(\phi_{ij}(\theta_{ij}) - \phi_{ij}(\theta_{ij,0}))/{\phi'}_{ij}(\theta_{ij,0}), \end{aligned} \tag{10}$$

$$\begin{aligned} Q_{ij}^L(\mathbf{f}_{ij}) = -b_{ij}[&(\varphi_i(v_i) - \varphi_i(v_{i,0}))/{\varphi'}_i(v_{i,0}) \\ &-(\varphi_j(v_j) - \varphi_j(v_{j,0}))/{\varphi'}_j(v_{j,0})] \\ &-g_{ij}(\phi_{ij}(\theta_{ij}) - \phi_{ij}(\theta_{ij,0}))/{\phi'}_{ij}(\theta_{ij,0}), \end{aligned} \tag{11}$$

with $\mathbf{f}_{ij} = (\varphi_i(v_i) = v_i^k, \varphi_j(v_j) = v_j^k, \phi_{ij}(\theta_{ij}) = \theta_{ij})^T, k \in N_+$ under the cold-start condition $(v_{i,0} = v_{j,0} = 1\ p.u., \theta_{ij,0} = 0)$. In addition, the form of $\mathbf{f}_{ij}$ can be not only selected as power function v_i^k. Reference [23] proposed a logarithmic linear power flow model with $\mathbf{f}_{ij} = (\varphi_i(v_i) = \ln v_i, \varphi_j(v_j) = \ln v_j, \phi_{ij}(\theta_{ij}) = \theta_{ij})^T$.

To further improve the linear power flow equation, several data-driven methods are proposed. Our previous work [24] guides the selection of $\mathbf{f}_{ij}$ by minimizing the linearization error of several historical scenarios. Reference [25] linearizes the power flow equation based on least squares regression. Reference [26] presents that the DC power flow model could be improved based on data-driven neural networks, but indicates that the black-box characteristic leads that neural-network-based approaches are hard to guarantee the security

of power system operation. Besides, reference [27] clarifies that the linear power equation is a lossless network model where the power losses should be compensated by considering the linearized quadratic components of v or θ. Reference [28] proposes a measurement of the maximum error of the linear power flow equations based on a volume of historical scenarios.

In addition, in practical solvers such as CPLEX, the piecewise linearization technique [29] and the iterative manner [30] are adopted to improve the accuracy at the expense of introducing integer variables or iterative steps. In a single piece or stage, these methods are still regarded as searching the more effective state space transformation $\mathbf{f}_{ij} = (\varphi_i(v_i), \varphi_j(v_j), \phi_{ij}(\theta_{ij}))^T$ based on empirical data.

Regarding the mathematical theory of linearization, Taylor series expansion is one of polynomial expansion techniques, which can only guarantee local accuracy around the initial point. To reduce errors within a specific range, we introduce the orthogonal polynomial expansion, which is derived based on minimizing the sum of squared errors of all feasible points in the operating bound [31]. The n-order Legendre polynomial on bound interval $[-1, 1]$ is shown as

$$T_n(x) = \frac{1}{2^n n!}\frac{d^n}{dx^n}\left(x^2-1\right)^n, x \in [-1,1], n \in N. \quad (12)$$

Legendre series is so-called orthogonal among the components of each order as shown in

$$\int_{-1}^{1} T_m(x)T_n(x)dx = \begin{cases} \frac{2}{2n+1}, m = n \\ 0, m \neq n \end{cases}, \quad (13)$$

Orthogonality reflects that the different components are integral-independent in the bound interval while the integral of the same component product is constant. It provides convenience for transforming any functions into the single Legendre variable space without empirical data. The arbitrary function $g(x)$ on interval $[-1, 1]$ can be easily expanded into Legendre polynomial series as shown in

$$g(x) = \sum_{n=0}^{\infty} A_n^g T_n(x), \quad (14)$$

where A_n^g is the magnitude of the n-order Legendre component. Based on orthogonality (13), A_n^g can be calculated according to

$$A_n^g = \frac{2n+1}{2}\int_{-1}^{1} g(x)T_n(x)dx. \quad (15)$$

So far, the arbitrary function $g(x)$ is transferred to Legendre independent variable space, where n-th dimension corresponds to the n-order Legendre component. It is a infinite polynomial series. Considering the limited computational source in practice, the components of all orders cannot be completely analyzed. Hence, the second-order Legendre series are employed to replace the infinite Legendre series in the following discussion. In fact, the component over second-order in power flow equations is extremely small and negligible, which is verified in case studies of section IV-A.

The characteristics of Taylor and Legendre polynomial expansions are compared in Fig. 1. The mathematical meaning of two expansion approaches is to transform the function into respective polynomial state spaces, where each dimension corresponds to a certain order component of Taylor or Legendre expansion. However, Taylor polynomial does not possess orthogonality like (13), whose magnitude of a certain order component cannot be conveniently derived according to (15) and is usually approximated through the expansion at the empirical operating point. Hence, Legendre polynomial expansion according to (14)-(15) has advantages in computational efficiency and accuracy within the entire operating bound.

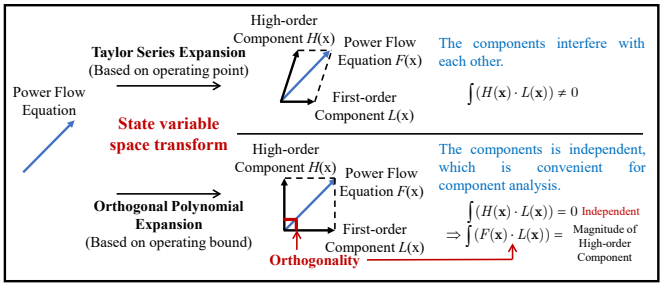

Fig. 1. Comparison of orthogonality of Taylor and Legendre polynomial expansions

In fact, there are several forms of orthogonal series. Without loss of generality, the commonly-used orthogonal polynomial series, Legendre polynomial series, are employed in the following discussion [32].

Taking the key nonlinear components in power flow equation (1)-(2), $\sin\theta_{ij}$ and $\cos\theta_{ij}$, as examples, the accuracies of their second-order Taylor and Legendre polynomial expansions (The derivation is shown in section II-A) are compared in Fig. 2. Considering the branch voltage angle difference in practical power systems satisfies $\theta_{ij} \in [-5°, 5°]$, Legendre polynomial expansion can well control the error within the entire operating bound. By comparison, Taylor series expansion might cause errors of more than three times when the operating state deviates from the initial point. In actual power dispatch where the security is the first priority, although the local error may be slightly worse than Taylor expansion, Legendre polynomial expansion guarantees that the global error of the scheduling result is within a secure range. It is worth noting, although the Legendre series is not linear, this does not prevent us from proposing a linear OPF model as shown in section III.

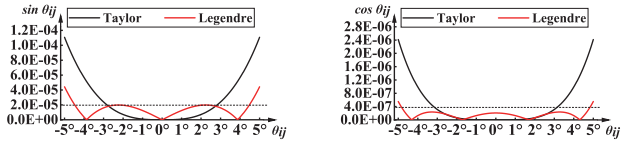

(a) $\sin\theta_{ij}$ (b) $\cos\theta_{ij}$

Fig. 2. Comparison of second-order Taylor and Legendre polynomial expansions of $\sin\theta_{ij}$ and $\cos\theta_{ij}$

C. Contributions

The contributions are summarized as follows:

1) A component analysis method to theoretically compare power flow equations in accuracy is proposed: The power flow equation (1)-(2) and its linear formulation (3)-(4) are expanded as Legendre polynomial series based on the operating bound. i.e., power flow equations are uniformly transformed into a single state variable space, where each dimension corresponds to a certain order component of Legendre expansion. Through comparing the magnitude of each order Legendre component, the improvement of linear power flow equations is revealed as the formulation of an appropriate state variable space transformation $\mathbf{f}_{ij} = (\varphi_i(v_i), \varphi_j(v_j), \phi_{ij}(\theta_{ij}))^T$ to reduce Legendre component loss. Based on this, the accuracy of the commonly used linear power flow equations are theoretically measured without historical knowledge.

2) The linear power flow equation minimizing Legendre component loss is proposed: An optimization model to obtain the linear power flow equation minimizing Legendre component loss is proposed. Considering the limited computing resources in practice, only finite-order components can be optimized. For compensating the inevitable component loss, we further derive the second-order component of the solved linear power flow equation. Based on the relaxation technique considering the operating bound, the second-order component is successfully modeled as linear constraints. The formulation of the solved linear power flow equation is only determined by network parameters, the operating bound rather than empirical operating data.

This paper is organized as follows. The component analysis of power flow equations is proposed in section II. The linear power flow equation minimizing Legendre component loss is proposed in section III. Case studies are presented in section IV, and section V concludes the paper.

II. Component Analysis of Power Flow Equations

The power flow equation (1)-(2) and its linear formulation (3)-(4) are transformed into a single state variable space based on Legendre polynomial expansion. Then, their accuracies are theoretically compared through component analysis in each dimension.

A. Legendre Polynomial Transformation of Power Flow Equations

In order to compare the power flow equations in the same state variable space, Legendre polynomial expansions of power flow equations are derived. Considering Legendre polynomials used in section I-B are defined on interval $[-1, 1]$, power flow equations is normalized by translating and scaling state variable $\mathbf{x}_{ij} = (v_i, v_j, \theta_{ij})^T$.

Firstly, the operating bound of power system can be directly constrained by a set of the box constraints as shown in

$$v_i \in [v_{i,0} - \Delta v_i, v_{i,0} + \Delta v_i], \theta_{ij} \in [-\Delta\theta_{ij}, \Delta\theta_{ij}], \quad (16)$$

where $i, j \in \mathcal{J}$, Δv_i and $\Delta\theta_{ij}$ are the maximum variation of state variables. The normalized state variable can be formulated as

$$x_{ij}^{norm} = (V_i, V_j, \Theta_{ij}), V_i, V_j, \Theta_{ij} \in [-1, 1], \quad (17)$$

where

$$V_i = \frac{v_i - v_{i,0}}{\Delta v_i}, \Theta_{ij} = \frac{\theta_{ij}}{\Delta\theta_{ij}}. \quad (18)$$

Then, we derive Legendre expansions of the original power flow equation (1)-(2) and its general linear formulation (3)-(4) as follows.

1) Legendre polynomial expansion of original power flow equation: Taking (18) into (1)-(2), the original power flow equation can be normalized as

$$\begin{aligned} P_{ij}(\mathbf{x}_{ij}^{norm}) &= g_{ij}(\Delta v_i^2 V_i^2 + v_{i,0}^2 + 2\Delta v_{i,0} v_{i,0} V_i) \\ &-(\Delta v_i V_i + v_{i,0})(\Delta v_j V_j + v_{j,0})[g_{ij}\cos(\Delta\theta_{ij}\Theta_{ij}) \\ &+b_{ij}\sin(\Delta\theta_{ij}\Theta_{ij})], \end{aligned} \quad (19)$$

$$\begin{aligned} Q_{ij}(\mathbf{x}_{ij}^{norm}) &= -b_{ij}(\Delta v_i^2 V_i^2 + v_{i,0}^2 + 2\Delta v_{i,0} v_{i,0} V_i) \\ &+(\Delta v_i V_i + v_{i,0})(\Delta v_j V_j + v_{j,0})[b_{ij}\cos(\Delta\theta_{ij}\Theta_{ij}) \\ &-g_{ij}\sin(\Delta\theta_{ij}\Theta_{ij})]. \end{aligned} \quad (20)$$

For obtaining Legendre polynomial expansion of the original power flow equation, the basic terms in (19)-(20) is firstly derived as Legendre polynomials according to (12) as shown as

$$V_i = T_1(V_i), V_j = T_1(V_j), \quad (21)$$

$$V_i^2 = \frac{1}{3}T_0(V_i) + \frac{2}{3}T_2(V_i), \quad (22)$$

$$\cos(\Delta\theta_{ij}\Theta_{ij}) = \sum_{n=0}^{\infty} A_{ij,n}^{\cos} T_n(\Theta_{ij}), \quad (23)$$

$$\sin(\Delta\theta_{ij}\Theta_{ij}) = \sum_{n=0}^{\infty} A_{ij,n}^{\sin} T_n(\Theta_{ij}), \quad (24)$$

where $A_{ij,n}^{cos}$ and $A_{ij,n}^{sin}$ are the magnitudes of the n-order components in $\cos(\Delta\theta_{ij}\Theta_{ij})$ and $\sin(\Delta\theta_{ij}\Theta_{ij})$. The derivation of $A_{ij,n}^{cos}$ and $A_{ij,n}^{sin}$ can be found in Appendix A. Taking (21)-(24) into (19)-(20), Legendre polynomial expansion of the power flow equation can be obtained. The second-order Legendre expansion of the power flow equation is written as

$$P_{ij}(\mathbf{x}_{ij}^{norm}) = \sum_{\substack{n_1+n_2+n_3\leq 2,\\ n_1,n_2,n_3\in N}} A_{ij,n_1n_2n_3}^{P} T_{n_1}(V_i) T_{n_2}(V_j) T_{n_3}(\Theta_{ij}), \quad (25)$$

$$Q_{ij}(\mathbf{x}_{ij}^{norm}) = \sum_{\substack{n_1+n_2+n_3\leq 2,\\ n_1,n_2,n_3\in N}} A_{ij,n_1n_2n_3}^{Q} T_{n_1}(V_i) T_{n_2}(V_j) T_{n_3}(\Theta_{ij}), \quad (26)$$

where $A_{ij,n_1n_2n_3}^{P}(n_1 + n_2 + n_3 \leq 2)$ is the magnitude of the $n_1n_2n_3$-order Legendre component of the original active power flow equation, as show in

$$A_{ij,000}^{P} = \frac{1}{3}g_{ij}\Delta v_i^2 + g_{ij}v_{i,0}^2 - g_{ij}v_{i,0}v_{j,0}A_0^{\cos}, \quad (27)$$

$$A_{ij,100}^{P} = 2g_{ij}\Delta v_i v_{i,0} - g_{ij}\Delta v_i v_{j,0}A_0^{\cos}, \quad (28)$$

$$A_{ij,010}^{P} = -g_{ij}\Delta v_j v_{i,0}A_0^{\cos}, \quad (29)$$

$$A_{ij,001}^{P} = -b_{ij}v_{i,0}v_{j,0}A_1^{\sin}, \quad (30)$$

$$A_{ij,200}^{P} = \frac{2}{3}g_{ij}\Delta v_i^2, \quad (31)$$

$$A_{ij,110}^{P} = -g_{ij}\Delta v_i \Delta v_j A_0^{\cos}, \quad (32)$$

$$A^{P}_{ij,101} = -b_{ij}\Delta v_i v_{j,0} A^{\sin}_1, \tag{33}$$

$$A^{P}_{ij,011} = -b_{ij}\Delta v_j v_{i,0} A^{\sin}_1, \tag{34}$$

$$A^{P}_{ij,002} = -g_{ij} v_{i,0} v_{j,0} A^{\cos}_2. \tag{35}$$

$A^{Q}_{ij,n_1n_2n_3}$ can be obtained by replacing g_{ij} and b_{ij} with $-b_{ij}$ and g_{ij} in (27)-(35).

2) Legendre polynomial expansion of linear power flow equations: The detailed formulation of the commonly-used linear power flow equation reviewed in section I-B can be written as (10)-(11) where the specific value of k represents the corresponding linear power flow equation based on the certain state space transformation $\mathbf{f}_{ij}$. Firstly, the basic terms $\varphi_i(v_i), \varphi_j(v_j), \phi_{ij}(\theta_{ij})$ are firstly normalized and expanded as

$$\varphi_i(v_i) = v_i^k = (\Delta v_i V_i + v_{i,0})^k = \sum_{n=0}^{\infty} A^{\varphi}_{i,n} T_n(V_i), \tag{36}$$

$$\varphi_j(v_j) = v_j^k = (\Delta v_j V_j + v_{j,0})^k = \sum_{n=0}^{\infty} A^{\varphi}_{j,n} T_n(V_j), \tag{37}$$

$$\phi_{ij}(\theta_{ij}) = \theta_{ij} = \Delta\theta_{ij}\Theta_{ij} = \Delta\theta_{ij} T_1(\Theta_{ij}), \tag{38}$$

where $A^{\varphi}_{i,n}, A^{\varphi}_{j,n}$ are the magnitudes of the n-order Legendre components in $\varphi_i(v_i)$ and $\varphi_j(v_j)$. Their derivation is presented in Appendix B. Taking (36)-(38) into (10)-(11), Legendre polynomial expansion of general linear power flow equation is obtained as shown in

$$P^{L}_{ij}(\mathbf{x}^{norm}_{ij}) = \sum_{\mathcal{N}} A^{P,L}_{ij,n_1n_2n_3} T_{n_1}(V_i) T_{n_2}(V_j) T_{n_3}(\Theta_{ij}), \tag{39}$$

$$Q^{L}_{ij}(\mathbf{x}^{norm}_{ij}) = \sum_{\mathcal{N}} A^{Q,L}_{ij,n_1n_2n_3} T_{n_1}(V_i) T_{n_2}(V_j) T_{n_3}(\Theta_{ij}), \tag{40}$$

where $\mathcal{N}$ is the set of component index of Legendre polynomials, m is the order number that can be considered under limited computation resource. It is worth noting, there is no cross-multiplied component of v_i, v_j, θ_{ij} in linear power flow equation (10)-(11). Thus, only when at least two of n_1, n_2 and n_3 is zero, the $n_1n_2n_3$-th Legendre component is non-zero. In addition, there only exists the first-order component of θ_{ij} in (10)-(11), i.e., Legendre component with $n_3 \geq 2$ is zero. The set of (n_1, n_2, n_3) with non-zero Legendre components is written as

$$\begin{aligned}\mathcal{N} = \{&(n_1,n_2,n_3)\,|(n_1,n_2,n_3) = (0,0,1)\,,(h,0,0)\\ &\text{or } (0,h,0), h \in N_+, h \leq m\},\end{aligned} \tag{41}$$

$A^{P,L}_{ij,n_1n_2n_3}, A^{Q,L}_{ij,n_1n_2n_3}$ are the magnitudes of the $n_1n_2n_3$-order component in $\mathcal{N}$. $A^{P,L}_{ij,n_1n_2n_3}$ is written as

$$A^{P,L}_{ij,000} = g_{ij}\frac{A^{\varphi}_{i,0}}{k} - g_{ij}\frac{A^{\varphi}_{j,0}}{k}, \tag{42}$$

$$A^{P,L}_{ij,001} = -b_{ij}\Delta\theta_{ij}, \tag{43}$$

$$A^{P,L}_{ij,n_100} = g_{ij}\frac{A^{\varphi}_{i,n_1}}{k}, \tag{44}$$

$$A^{P,L}_{ij,0n_20} = -g_{ij}\frac{A^{\varphi}_{j,n_1}}{k}. \tag{45}$$

$A^{Q,L}_{ij,n_1n_2n_3}$ can be obtained by replacing g_{ij} and b_{ij} with $-b_{ij}$ and g_{ij} in (42)-(45).

So far, power flow equations are transformed into the same Legendre state variable space.

B. Component Analysis of Power Flow Equations

Power flow equations are compared in Legendre state variable space based on component analysis. The conclusion will draw that the improvement of linear power flow equations is to formulate an appropriate state variable space transformation $\mathbf{f}_{ij}$ to reduce Legendre component loss.

Firstly, we focus on comparing the original power flow equation, its basic linearized formulation (10)-(11) with $k = 1$, and the improved linear model (10)-(11) with $k = 2$, where the latter two are the widely-used linear power flow models in power industry. The DC power flow equation can be regard as a special formulation of (10)-(11) with $k = 1$ under the assumption that $r_{ij}/x_{ij} \approx 0$.

Taking active power as an example, the active power flow equation (39) with $k = 1, 2$ is written as

$$\begin{aligned}P^{k=1}_{ij}(\mathbf{x}^{norm}_{ij}) = {}& g_{ij}\Delta v_i T_1(V_i) - g_{ij}\Delta v_j T_1(V_j)\\ &- b_{ij}\Delta\theta_{ij} T_1(\phi_{ij}),\end{aligned} \tag{46}$$

$$\begin{aligned}P^{k=2}_{ij}(\mathbf{x}^{norm}_{ij}) = {}& g_{ij}\Delta v_i v_{i,0} T_1(V_i) - g_{ij}\Delta v_j v_{j,0} T_1(V_j)\\ &- b_{ij}\Delta\theta_{ij} T_1(\phi_{ij}) + \tfrac{1}{3} g_{ij}\Delta {v_i}^2 T_2(V_i) - \tfrac{1}{3} g_{ij}\Delta {v_j}^2 T_2(V_j),\end{aligned} \tag{47}$$

Comparing models (46)-(47) with transformed original power flow equation (25), model (46) approximates the first-order component of the original power flow equation, i.e., the magnitudes of first-order dimensions $T_1(V_i)$, $T_1(V_j)$ and $T_1(\phi_{ij})$ are approximately remained in the Legendre state variable space; model (47) approximates not only the first-order but also the second-order components, where the second-order dimensions are $T_2(V_i)$ and $T_2(V_j)$. Compared with the magnitude of each order component in original power flow equation (25), the absolute errors when $k = 1$ in second-order dimensions $T_2(V_i)$ and $T_2(V_j)$ are shown as

$$\Delta A^{P,k=1}_{ij,200} = 2\,|g_{ij}|\,\Delta v_i^2/3, \tag{48}$$

$$\Delta A^{P,k=1}_{ij,020} = 0, \tag{49}$$

The absolute errors when $k = 2$ in second-order dimensions $T_2(V_i)$ and $T_2(V_j)$ are shown as

$$\Delta A^{P,k=2}_{ij,200} = |g_{ij}|\,\Delta v_i^2/3, \tag{50}$$

$$\Delta A^{P,k=2}_{ij,020} = |g_{ij}|\,\Delta {v_j}^2/3, \tag{51}$$

The operating bound of voltage magnitude on adjacent buses i and j are usually set equal ($\Delta v_i = \Delta v_j$). Thus, it is easy to derived, in the second-order dimensions of the state variable space, the module variance when $k = 2$ is smaller than that when $k = 1$ as shown in

$$\left(\Delta A^{P,k=1}_{ij,200}\right)^2 + \left(\Delta A^{P,k=1}_{ij,020}\right)^2 > \left(\Delta A^{P,k=2}_{ij,200}\right)^2 + \left(\Delta A^{P,k=2}_{ij,020}\right)^2. \tag{52}$$

Since the reactive power equation can be formulated only by replacing g_{ij} and b_{ij} with $-b_{ij}$ and g_{ij} in the active power flow equation according to (1)-(2), the reactive and active power

have similar formulations and holds same conclusions. Hence, compared with the situation with $k = 1$, the improvement of linear power flow equations is to select an appropriate state variable space transformation $\mathbf{f}_{ij} = (v_i^k, v_j^k, \theta_{ij})^T$ with $k = 2$ to reduce the second-order Legendre component loss. In addition, there exists linear power flow models with different form of $\mathbf{f}_{ij}$, such as the mentioned logarithmic form in section I-B. They can be analyzed and compared based on the above process. In the following discussion, we focus on the situation with $\mathbf{f}_{ij} = (v_i^k, v_j^k, \theta_{ij})^T$. Further, we extend the value of k from positive integers set N_+ to positive real number set R_+. Theoretically, the optimal formulation of the power flow equation corresponds to the form of $\mathbf{f}_{ij}$ minimizing Legendre component loss.

III. Linear Power Flow Equation Minimizing Legendre Component Loss

An optimization model is proposed to solve the linear power flow equation minimizing Legendre component loss under the specific operating bound $\Delta v_i, \Delta v_j$ and $\Delta\theta_{ij}$, as shown as

$$\min \sum_{\mathcal{B}} F_{ij}(k, \Delta v_i, \Delta v_j, \Delta\theta_{ij}), \tag{53}$$

where $\mathcal{B}$ is the set of all branches in the power system. We assume that the losses of all Legendre components have same weight. $F_{ij}(k, \Delta v_i, \Delta v_j, \Delta\theta_{ij})$ are the sum of quadratic magnitude deviations on branch $\{ij\}$ as

$$\begin{aligned} F_{ij}(k, \Delta v_i, \Delta v_j, \Delta\theta_{ij}) &= \sum_{\mathcal{N}} \left(\Delta A^P_{ij,n_1n_2n_3}\right)^2 \\ &+ \sum_{\mathcal{N}} \left(\Delta A^Q_{ij,n_1n_2n_3}\right)^2, \{ij\} \in \mathcal{B}, \end{aligned} \tag{54}$$

in which $\Delta A^P_{ij,n_1n_2n_3}$ and $\Delta A^Q_{ij,n_1n_2n_3}$ are the linearization deviation of the magnitude of $n_1n_2n_3$-order Legendre component, i.e., the $n_1n_2n_3$-th order Legendre component losses, which is written as

$$\Delta A^P_{ij,n_1n_2n_3} = A^P_{ij,n_1n_2n_3} - A^{P,L}_{ij,n_1n_2n_3}, \tag{55}$$

$$\Delta A^Q_{ij,n_1n_2n_3} = A^Q_{ij,n_1n_2n_3} - A^{Q,L}_{ij,n_1n_2n_3}, \tag{56}$$

$A^P_{ij,n_1n_2n_3}$ and $A^{P,L}_{ij,n_1n_2n_3}$ are written as (27)-(35) and (42)-(45). $A^Q_{ij,n_1n_2n_3}$ and $A^{Q,L}_{ij,n_1n_2n_3}$ is derived by replacing g_{ij} and b_{ij} with $-b_{ij}$ and g_{ij} in the formulations of $A^P_{ij,n_1n_2n_3}$ and $A^{P,L}_{ij,n_1n_2n_3}$.

k is the decision variable. The solved value of k is determined by the operating bound $\Delta v_i, \Delta v_j, \Delta\theta_{ij}$ and physical parameter b_{ij}, g_{ij} in the certain power system. It is independent with history operating data. In practice, the optimization process can be executed offline. When the operating state changes dramatically, the linear power flow model can be updated by re-executing the optimization model (53). In this paper, we consider problem (53) is an unconstrained optimization problem, which can be solved based on CPLEX. The objective is piecewise linearized into 5000 segments based on the default piecewise linearization function. The solution and performance of the proposed linear power flow model is verified in case studies of section IV. In addition, noting that k can be also selected based on historical data. For example, reference [24] proposes an approach for solving the value of k by minimizing the sum of squared errors of the branch power flow in historical OPF scenarios. However, practical statistical information might be insufficient. Even if sufficient, the method proposed in this paper can also more precisely determine the operating bound based on historical data to improve the accuracy of the solved linear power flow model. Thus, the proposed method is suitable for more general practical scenarios.

For further discussion, we donate the solved value of k as κ. Taking $\mathbf{f}_{ij} = (v_i^\kappa, v_j^\kappa, \theta_{ij})^T$ into (10)-(11), the solved linear power flow equation is formulated as

$$P^{L,S}_{ij} = g_{ij}(\varphi_i - \varphi_j)/\kappa - b_{ij}\theta_{ij}, \tag{57}$$

$$Q^{L,S}_{ij} = -b_{ij}(\varphi_i - \varphi_j)/\kappa - g_{ij}\theta_{ij}, \tag{58}$$

where φ_i, φ_j are transformed state variables, v_i and v_j can be solved through $v_i = (\varphi_i)^{-\kappa}$. Hence, the nonlinearity of the state-space transformation $\mathbf{f}_{ij} = (v_i^\kappa, v_j^\kappa, \theta_{ij})^T$ is not included in the OPF model, but only appears in the simple inverse operation of the OPF result.

However, considering the computational efficiency in practice, the optional form of $\mathbf{f}_{ij}$ is limited. This will cause some state-space transformation cannot be selectable, resulting in the inevitable loss of high-order components. Noting that Legendre polynomial expansion employs operating bound information, we further provide an operating-bound-based approach for compensating the second-order components, which is easy to be extended to higher order.

Firstly, it is observed that the solved linear power flow equation (57)-(58) is the first-order Taylor expansion of the original power flow equation (1)-(2) with state variable transformation $\mathbf{f}_{ij} = (v_i^\kappa, v_j^\kappa, \theta_{ij})^T$. The lost Legendre components are included in the high-order Taylor expansion. The second-order Taylor expansion of (1)-(2) with $\mathbf{f}_{ij} = (v_i^\kappa, v_j^\kappa, \theta_{ij})^T$ under the cold-start condition can be formulated as

$$\begin{aligned} P^{H,S}_{ij} &= (\tfrac{3}{2\kappa^2} - \tfrac{1}{2\kappa})g_{ij}H_{ij,11} - (\tfrac{1}{2\kappa^2} - \tfrac{1}{2\kappa})g_{ij}H_{ij,22} \\ &+ \tfrac{1}{2}g_{ij}H_{ij,33} - \tfrac{1}{\kappa^2}g_{ij}H_{ij,12} - \tfrac{1}{\kappa}b_{ij}H_{ij,13} - \tfrac{1}{\kappa}b_{ij}H_{ij,23} \\ &- (\tfrac{2}{\kappa^2} - \tfrac{1}{\kappa})g_{ij}\varphi_i + (\tfrac{2}{\kappa^2} - \tfrac{1}{\kappa})g_{ij}\varphi_j, \end{aligned} \tag{59}$$

$$\begin{aligned} Q^{H,S}_{ij} &= -(\tfrac{3}{2\kappa^2} - \tfrac{1}{2\kappa})b_{ij}H_{ij,11} + (\tfrac{1}{2\kappa^2} - \tfrac{1}{2\kappa})b_{ij}H_{ij,22} \\ &- \tfrac{1}{2}b_{ij}H_{ij,33} + \tfrac{1}{\kappa^2}b_{ij}H_{ij,12} - \tfrac{1}{\kappa}g_{ij}H_{ij,13} - \tfrac{1}{\kappa}g_{ij}H_{ij,23} \\ &+ (\tfrac{2}{\kappa^2} - \tfrac{1}{\kappa})b_{ij}\varphi_i - (\tfrac{2}{\kappa^2} - \tfrac{1}{\kappa})b_{ij}\varphi_j, \end{aligned} \tag{60}$$

where $H_{ij,l_1l_2}(l_1, l_2 = 1, 2, 3)$ are the product of two state variables as shown in

$$\begin{aligned} H_{ij,l_1l_2} &= f_{ij,l_1}f_{ij,l_2} \\ (l_1, l_2 = 1, 2, 3; \mathbf{f}_{ij} = (\varphi_i, \varphi_j, \theta_{ij}) &\overset{define}{=} (f_{ij,1}, f_{ij,2}, f_{ij,3})), \end{aligned} \tag{61}$$

Regarding H_{ij,l_1l_2} as relaxed state variables, the second-order component (59)-(60) is still linear. The nonlinearity is only presented in (61). We employ reformulation linearization technique (RLT) [33] to linearize (61) based on the operating bound of f_{ij,l_1}. Taking (16) into $\mathbf{f}_{ij} = (v_i^\kappa, v_j^\kappa, \theta_{ij})^T$, the operating bound of f_{ij,l_1} can be easily defined as

$$f_{ij,l_1} \in [f^{\min}_{ij,l_1}, f^{\max}_{ij,l_1}], l_1 = 1, 2, 3, \tag{62}$$

The basic idea of RLT is to envelope H_{ij,l_1l_2} with a set of linear constraints. Taking $H_{ij,l_1l_2} = v_i^2$ (monotonic) and θ_{ij}^2 (non-monotonic) as examples, the envelopes of monotonic and non-monotonic functions can be constructed as the yellow area in Fig. 3. Besides, considering H_{ij,l_1l_2} are quadratic functions, we further tighten the envelope of non-monotonic quadratic functions as the shaded area in Fig. 3(b).

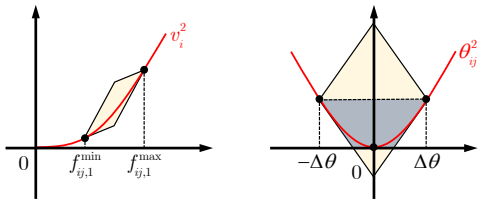

(a) v_i^2 (b) θ_{ij}^2

Fig. 3. RLT process on v_i^2 and θ_{ij}^2

Hence, regarding the monotonic functions in the set of $H_{ij,l_1l_2}(l_1 \neq l_2)$, constraint (61) can be relaxed as

$$\begin{cases} H_{ij,l_1l_2} \geq f_{ij,l_1}^{\min} f_{ij,l_2} + f_{ij,l_2}^{\min} f_{ij,l_1} - f_{ij,l_1}^{\min} f_{ij,l_2}^{\min} \\ H_{ij,l_1l_2} \geq f_{ij,l_1}^{\max} f_{ij,l_2} + f_{ij,l_2}^{\max} f_{ij,l_1} - f_{ij,l_1}^{\max} f_{ij,l_2}^{\max} \\ H_{ij,l_1l_2} \leq f_{ij,l_1}^{\min} f_{ij,l_2} + f_{ij,l_2}^{\max} f_{ij,l_1} - f_{ij,l_1}^{\min} f_{ij,l_2}^{\max} \\ H_{ij,l_1l_2} \leq f_{ij,l_1}^{\max} f_{ij,l_2} + f_{ij,l_2}^{\min} f_{ij,l_1} - f_{ij,l_1}^{\max} f_{ij,l_2}^{\min} \end{cases}. \quad (63)$$

Regarding the non-monotonic quadratic functions in the set of $H_{ij,l_1l_2}(l_1 = l_2)$, constraint (61) can be relaxed as

$$\begin{cases} H_{ij,l_1l_2} \geq f_{ij,l_1}^{\min} f_{ij,l_2} + f_{ij,l_2}^{\min} f_{ij,l_1} - f_{ij,l_1}^{\min} f_{ij,l_2}^{\min} \\ H_{ij,l_1l_2} \geq f_{ij,l_1}^{\max} f_{ij,l_2} + f_{ij,l_2}^{\max} f_{ij,l_1} - f_{ij,l_1}^{\max} f_{ij,l_2}^{\max} \\ H_{ij,l_1l_2} \geq 0 \\ H_{ij,l_1l_2} \leq \frac{(f_{ij,l_1}^{\max})^2 - (f_{ij,l_1}^{\min})^2}{f_{ij,l_1}^{\max} - f_{ij,l_1}^{\min}} (f_{ij,l_1} - f_{ij,l_1}^{\min}) + (f_{ij,l_1}^{\min})^2 \end{cases}. \quad (64)$$

It is worth noting, the n-order Taylor components can be constructed as the product of two $(n-1)$-order components. Hence, the constraints (61) of the higher-order components and its RLT constraints can be iteratively formulated based on the RLT model of lower-order components. In this paper, the second-order component loss compensation is adopted and verified in case studies.

So far, we summarize the algorithm for solving the linear power flow model minimizing the component loss and the application in OPF calculation, as shown in the following steps:

Step1: Operating bound $\Delta v_i, \Delta v_j, \Delta\theta_{ij}$ is determined according to accuracy and operating demand. Model (53)-(56) is executed to solve the value of κ. Equation (57)-(58) with the solved κ is the proposed linear power flow equation before component compensation.

Step2: The second-order component is compensated into the solved linear power flow equation. The power flow equation is reformulated as shown in

$$P_{ij}^{RL} = P_{ij}^{L,S} + P_{ij}^{H,S}, \quad (65)$$

$$Q_{ij}^{RL} = Q_{ij}^{L,S} + Q_{ij}^{H,S}, \quad (66)$$

where $P_{ij}^{L,S}$ and $Q_{ij}^{L,S}$ is shown as (57)-(58), $P_{ij}^{H,S}$ and $Q_{ij}^{H,S}$ is shown as (59)-(60).

Step3: The linear power flow equation (65)-(66) and the corresponding constraints (63) or (64) caused by the relaxation variable H_{ij,l_1l_2} are added into OPF model. The linear OPF model is obtained.

IV. Case Studies

3000 OPF results (1000 for each system) of IEEE 30, 118 and Polish 2383 benchmark systems with 20% load fluctuation are used to verify the proposed method, where the basic scenario with 0% load fluctuation are based on the default operating data of Matpower 6.0. The load dataset of the 3000 samples is provide in [34]. The computations are performed using GAMS on a computer with a Core i5–9300H CPU. The linear power flow equations (6)-(7) ($k = 1$), (8)-(9) ($k = 2$), proposed (57)-(58) ($k = \kappa$ before component compensation) and proposed (57)-(58) ($k = \kappa$ after component compensation (63)-(64)) are compared with original AC power flow equation (1)-(2), where the solved value of κ is $\kappa = 1.74$ in IEEE 30 test system, $\kappa = 2.15$ in IEEE 118 test system and $\kappa = 1.97$ in Polish 2383 test system. It is worth noting, the MW-only DC power flow equation is a simplified version with $k = 1$ (as shown in section I-B) so that it is not listed separately in case studies.

A. Legendre Component Loss of Linear Power Flow Equations

For accurately calculating the Legendre component loss in each OPF scenario, we ideally set that the operating bound is around the OPF result, i.e., $\Delta v_i = |v_i - v_{i,0}|, \Delta\theta_{ij} = |\theta_{ij} - \theta_{ij,0}|$ where v_i, θ_{ij} represent the solved state variable in OPF results. Although this ideal bound setting cannot be actually implemented in practice, it can be used to improve the accuracy of component loss evaluation after the OPF model is solved due that the bounds of the Legendre polynomial expansion are more precise. The initial state is under cold-start condition ($v_{i,0} = 1\ p.u.$ and $\theta_{ij,0} = 0$). Since Legendre component loss of the linear power flow equation is uniformly the deviation of the branch power flow, they take the same weight. The n-order component loss can be measured as the sum of the n-order absolute error, as shown in

$$\Delta P_{ij}^{o=n} = \sum_{n_1+n_2+n_3=n} \left|\Delta A_{ij,n_1n_2n_3}^{P}\right|, \quad (67)$$

$$\Delta Q_{ij}^{o=n} = \sum_{n_1+n_2+n_3=n} \left|\Delta A_{ij,n_1n_2n_3}^{Q}\right|. \quad (68)$$

The proportion of the n-order Legendre component loss in the branch power flow can be formulated as

$$e_n^P = \frac{\sum_B \Delta P_{ij}^{o=n}}{\sum_B |P_{ij}|} \times 100\%, \quad (69)$$

$$e_n^Q = \frac{\sum_B \Delta Q_{ij}^{o=n}}{\sum_B |Q_{ij}|} \times 100\%. \quad (70)$$

The average proportion of the n-order Legendre component loss, e_n^P and e_n^Q, in 3000 OPF samples are shown in Fig. 4. Comparing the different order components in each model,

TABLE I
AVERAGE AND MAXIMUM ERROR OF POWER GENERATION IN 3000 STAGES

IEEE & Polish Test System	$(P_i - P_{i,L})/P_i \times 100\%$ (Unit: %)								$(Q_i - Q_{i,L})/Q_i \times 100\%$ (Unit: %)							
	$k=1$		$k=2$		$k=\kappa$ before compensation		$k=\kappa$ before compensation		$k=1$		$k=2$		$k=\kappa$ before compensation		$k=\kappa$ before compensation	
	Avg	Max	Avg	Max	Avg	Max	Avg	Max	Avg	Max	Avg	Max	Avg	Max	Avg	Max
30	6.8	13.1	4.8	12.9	3.1	8.0	1.3	3.4	42.2	47.5	42.8	47.8	26.5	33.7	8.7	9.7
118	4.5	4.6	2.6	2.7	1.2	3.2	0.5	1.4	30.3	30.4	29.8	30.0	27.6	27.7	9.7	11.0
2383	9.3	13.5	9.1	13.1	4.4	7.4	4.0	7.0	19.3	22.0	13.4	15.6	13.3	15.4	5.6	6.6

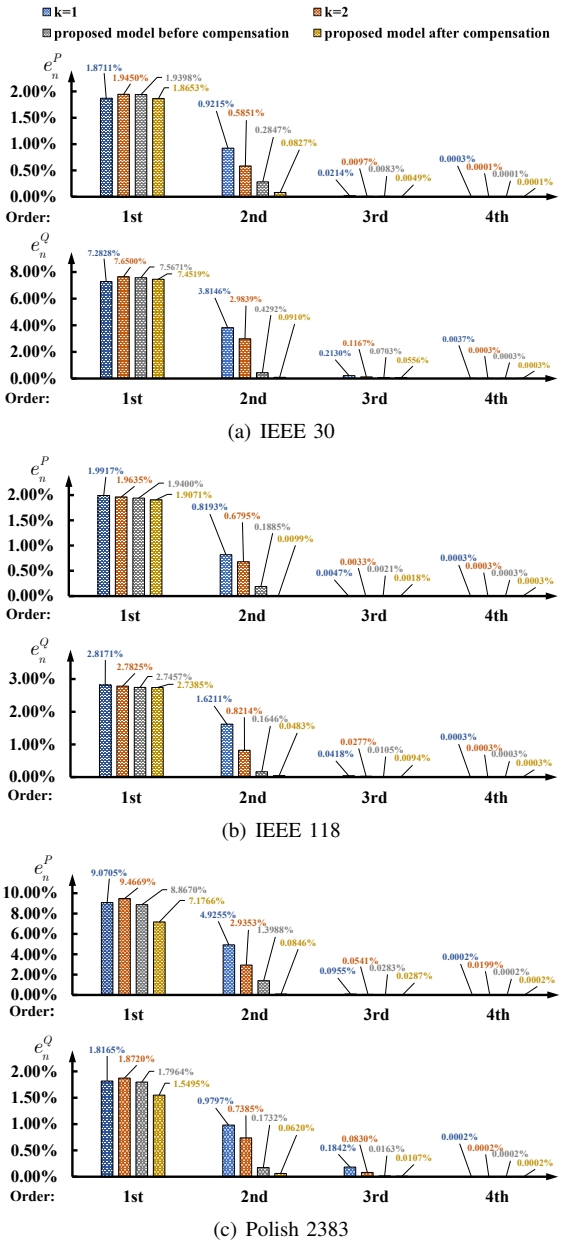

(a) IEEE 30

(b) IEEE 118

(c) Polish 2383

Fig. 4. The proportion of the n-order ($n = 1, 2, 3, 4$) Legendre component loss e_n^P and e_n^Q in 3000 OPF results

e_n^P and e_n^Q present a rapid downward trend as the number of orders rises. In practical calculation scenarios, the components of the third and fourth orders can be neglected, whose losses are less than 5% of the first and second orders. Comparing the different models in each component, in the first order, the four models almost produced the similar component loss; in the second order, the model with $k = 2, \kappa$ before component compensation and $k = \kappa$ after component compensation can reduce the component loss with $k = 1$ by about 30%, over 65% and over 90%, respectively. Hence, the proposed linear power flow model notably reduces the loss of the second-order Legendre component. It will improve the accuracy of the linear power flow equation, which is verified in section IV-B.

TABLE II
PROPORTIONS OF INFEASIBLE SAMPLES

IEEE & Polish Test System	Proportions of Infeasible Samples (Unit: %)			
	$k=1$	$k=2$	$k=\kappa$ before compensation	$k=\kappa$ before compensation
30	21.0%	14.8%	9.2%	3.3%
118	15.0%	12.1%	9.5%	3.4%
2383	16.4%	11.4%	7.5%	5.9%

B. Real Time OPF Solutions in 3000 Stages

The Real Time OPF (RTOPF) results of the four power flow models in 3000 stages (1000 for each system) with 20% load fluctuation is compared. The computational time interval of each stage is set as 1.0 seconds to meet the demand in second-level power dispatch. The average error of active and reactive power generation in each stage is present in Fig. 5. Compared with the model with $k = 1$ and 2, the model with $k = \kappa$ before and after compensation reduces the active power error by about 50%, 80% and the reactive power error by 40%, 80%. The average and maximum errors of the active and reactive power generation in 3000 stages are shown in Table I. Compared with the model with $k = 1$ and 2, the model with $k = \kappa$ before and after compensation reduces the average error of the active power by 53.6%, 72.7%, the average error of the reactive power by 29.6%, 60.0%, the maximum error of the active power by 20.6%, 70.6% and the maximum error of the reactive power by 17.7%, 69.0%. Noting the conclusion in section IV-A, the accuracy of the OPF model present a positive correlation with the second-order component loss.

Besides, in these 3000 stages, several samples are unable to converge within the required computation time (1s), which are denoted as infeasible samples. These samples are marked as the point with corresponding colors on the curve in Fig. 5. The proportions of the infeasible points in four models are shown in Table II. The convergence performance improves by 31.1% before compensation and 65.9% after compensation.

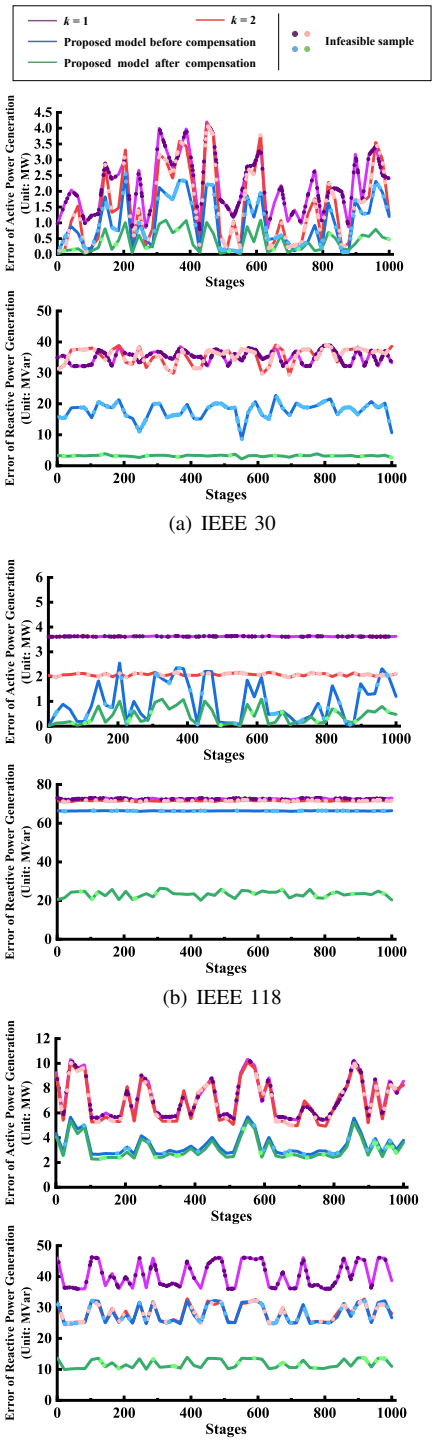

(a) IEEE 30

(b) IEEE 118

(c) Polish 2383

Fig. 5. The average error of active and reactive power generation in 3000 OPF results

V. Conclusion

In this paper, a linear power flow equation minimizing Legendre component loss is proposed. It provides a theoretical guidance for the linearization of the power flow equation without empirical data. The accuracy performance of the proposed model notably outperforms typical linear power flow models (with $k = 1$ and $k = 2$). However, this paper just employs one of orthogonal polynomials, Legendre series, as the modeling basis. Other orthogonal polynomials such as Chebyshev polynomial is worth compared in future study. Besides, the component analysis of general linear power flow models with more form of $\mathbf{f}_{ij}$ or under the complex operating region also deserves further discussion.

Appendix A
Legendre Polynomial Expansion of $\cos(\Delta\theta_{ij}\Theta_{ij})$ and $\sin(\Delta\theta_{ij}\Theta_{ij})$

In (23)-(24), $A_{ij,n}^{cos}$ and $A_{ij,n}^{sin}$ are the magnitudes of the n-order Legendre polynomials. Taking $n = 0, 1, 2$ as examples, $A_{ij,n}^{cos}$ and $A_{ij,n}^{sin}$ can be derived based on (14), as shown in

$$\begin{aligned} A_{ij,0}^{\cos} &= \tfrac{1}{2}\int_{-1}^{1}\cos(\Delta\theta_{ij}\Theta_{ij})T_0(\Theta_{ij})d\Theta_{ij} \\ &= \tfrac{1}{2}\int_{-1}^{1}\cos(\Delta\theta_{ij}\Theta_{ij})d\Theta_{ij} = \tfrac{\sin\Delta\theta_{ij}}{\Delta\theta_{ij}}, \end{aligned} \tag{71}$$

$$\begin{aligned} A_{ij,1}^{\cos} &= \tfrac{3}{2}\int_{-1}^{1}\cos(\Delta\theta_{ij}\Theta_{ij})T_1(\Theta_{ij})d\Theta_{ij} \\ &= \tfrac{3}{2}\int_{-1}^{1}\cos(\Delta\theta_{ij}\Theta_{ij})\Theta_{ij}d\Theta_{ij} \overset{parity}{=} 0, \end{aligned} \tag{72}$$

$$\begin{aligned} A_{ij,2}^{\cos} &= \tfrac{5}{2}\int_{-1}^{1}\cos(\Delta\theta_{ij}\Theta_{ij})T_2(\Theta_{ij})d\Theta_{ij} \\ &= \tfrac{5}{2}\int_{-1}^{1}\cos(\Delta\theta_{ij}\Theta_{ij})(\tfrac{3}{2}{\Theta_{ij}}^2 - \tfrac{1}{2})d\Theta_{ij} \\ &= \tfrac{15}{4}\int_{-1}^{1}\cos(\Delta\theta_{ij}\Theta_{ij}){\Theta_{ij}}^2 d\Theta_{ij} - \tfrac{5}{2}A_0^{\cos} \\ &= \tfrac{15}{4\Delta\theta_{ij}}\int_{-1}^{1}{\Theta_{ij}}^2 d\sin(\Delta\theta_{ij}\Theta_{ij}) - \tfrac{5}{2}A_0^{\cos} \\ &= \tfrac{15}{2}(\tfrac{\sin\Delta\theta_{ij}}{\Delta\theta_{ij}} + \tfrac{2\cos\Delta\theta_{ij}}{{\Delta\theta_{ij}}^2} - \tfrac{2\sin\Delta\theta_{ij}}{{\Delta\theta_{ij}}^3}) - \tfrac{5}{2}A_0^{\cos}, \end{aligned} \tag{73}$$

$$\begin{aligned} A_{ij,0}^{\sin} &= \tfrac{1}{2}\int_{-1}^{1}\sin(\Delta\theta_{ij}\Theta_{ij})T_0(\Theta_{ij})d\Theta_{ij} \\ &= \tfrac{1}{2}\int_{-1}^{1}\sin(\Delta\theta_{ij}\Theta_{ij})d\Theta_{ij} \overset{parity}{=} 0, \end{aligned} \tag{74}$$

$$\begin{aligned} A_{ij,1}^{\sin} &= \tfrac{3}{2}\int_{-1}^{1}\sin(\Delta\theta_{ij}\Theta_{ij})T_1(\Theta_{ij})d\Theta_{ij} \\ &= \tfrac{3}{2}\int_{-1}^{1}\sin(\Delta\theta_{ij}\Theta_{ij})\Theta_{ij}d\Theta_{ij} \\ &= -\tfrac{3\cos\Delta\theta_{ij}}{\Delta\theta_{ij}} + \tfrac{3\sin\Delta\theta_{ij}}{{\Delta\theta_{ij}}^2}, \end{aligned} \tag{75}$$

$$\begin{aligned} A_{ij,2}^{\sin} &= \tfrac{5}{2}\int_{-1}^{1}\sin(\Delta\theta_{ij}\Theta_{ij})T_2(\Theta_{ij})d\Theta_{ij} \\ &= \tfrac{5}{2}\int_{-1}^{1}\sin(\Delta\theta_{ij}\Theta_{ij})(\tfrac{3}{2}{\Theta_{ij}}^2 - \tfrac{1}{2})d\Theta_{ij} \overset{parity}{=} 0. \end{aligned} \tag{76}$$

$A_{ij,n}^{cos}$ and $A_{ij,n}^{sin}(n \geq 2)$ can be obtained in a similar way.

Appendix B
Legendre Polynomial Expansion of $\varphi_i(v_i) = v_i^k$

In (36)-(37), $A_{i,n}^{\varphi}$ and $A_{j,n}^{\varphi}$ are the magnitudes of the n-order Legendre components in $\varphi_i(v_i)$ and $\varphi_j(v_j)$. Taking $n = 0, 1, 2$ as examples, $A_{i,n}^{\varphi}$ and $A_{j,n}^{\varphi}$ can be derived based on (14), as shown in

$$\begin{aligned} A_{i,0}^{\varphi} &= \tfrac{1}{2}\int_{-1}^{1}(\Delta v_i V_i + v_{i,0})^k dV_i \\ &= \tfrac{1}{2\Delta v_i(k+1)}\left[(v_{i,0} + \Delta v_i)^{k+1} - (v_{i,0} - \Delta v_i)^{k+1}\right] \end{aligned} \tag{77}$$

$$\begin{aligned} A_{i,1}^{\varphi}(k, \Delta v_i) &= \tfrac{3}{2\Delta v_i}\int_{-1}^{1}[(\Delta v_i V_i + v_{i,0})^{k+1} \\ &-(\Delta v_i V_i + v_{i,0})^k v_{i,0}]dV_i \\ &= \tfrac{3}{2\Delta {v_i}^2(k+2)}\{[(v_{i,0} + \Delta v_i)^{k+2} \\ &-(v_{i,0} - \Delta v_i)^{k+2}] - \tfrac{3v_{i,0}}{\Delta v_i}A_0\} \end{aligned} \tag{78}$$

$A_{i,n}^{\varphi}(n \geq 2)$ can be obtained in a similar way. $A_{j,n}^{\varphi}$ can be obtained by replacing index "i" with index "j".

REFERENCES

[1] D. Bertsimas, E. Litvinov, X. A. Sun, J. Zhao, and T. Zheng, "Adaptive robust optimization for the security constrained unit commitment problem," *IEEE Trans. Power Syst.*, vol. 28, no. 1, pp. 52–63, 2013.

[2] H. Sun, Q. Li, M. Zhang, B. Wang, Q. Guo, and B. Zhang, "Continuation power flow method based on dynamic power flow equation," *Proc. CSEE*, vol. 31, no. 7, pp. 77–82, 2011.

[3] R. Jabr, "Optimal placement of capacitors in a radial network using conic and mixed integer linear programming," *Electr. Power Syst. Res.*, vol. 78, no. 6, pp. 941–948, 2008.

[4] D. Cao, W. Hu, X. Xu, Q. Wu, Q. Huang, Z. Chen, and F. Blaabjerg, "Deep reinforcement learning based approach for optimal power flow of distribution networks embedded with renewable energy and storage devices," *J. Mod. Power Syst. Clean Energy*, vol. 9, no. 5, pp. 1101–1110, 2021.

[5] M. B. Cain, R. P. O'neill, A. Castillo *et al.*, "History of optimal power flow and formulations," *Federal Energy Regulatory Commission*, vol. 1, pp. 1–36, 2012.

[6] M. Lubin, Y. Dvorkin, and S. Backhaus, "A robust approach to chance constrained optimal power flow with renewable generation," *IEEE Trans. Power Syst.*, vol. 31, no. 5, pp. 3840–3849, 2015.

[7] Y. Xu, Z. Liu, F. Wen, and I. Palu, "Receding-horizon based optimal dispatch of virtual power plant considering stochastic dynamic of photovoltaic generation," *Energy Convers. Econ.*, vol. 2, no. 1, pp. 45–53, 2021.

[8] F. Z. Peng, "Flexible ac transmission systems (facts) and resilient ac distribution systems (racds) in smart grid," *Proc. IEEE*, vol. 105, no. 11, pp. 2099–2115, 2017.

[9] H. Husin, M. Zaki *et al.*, "A critical review of the integration of renewable energy sources with various technologies," *Prot. Control Mod. Power Syst.*, vol. 6, no. 1, pp. 1–18, 2021.

[10] A. Karapetyan, M. Khonji, S. C.-K. Chau, K. Elbassioni, H. Zeineldin, T. H. EL-Fouly, and A. Al-Durra, "A competitive scheduling algorithm for online demand response in islanded microgrids," *IEEE Trans. Power Syst.*, vol. 36, no. 4, pp. 3430–3440, 2020.

[11] P. Pinson, H. Madsen *et al.*, "Benefits and challenges of electrical demand response: A critical review," *Renew. Sust. Energ. Rev.*, vol. 39, pp. 686–699, 2014.

[12] X. Kuang, B. Ghaddar, J. Naoum-Sawaya, and L. F. Zuluaga, "Alternative lp and socp hierarchies for acopf problems," *IEEE Trans. Power Syst.*, vol. 32, no. 4, pp. 2828–2836, 2017.

[13] Z. Yang, K. Xie, J. Yu, H. Zhong, N. Zhang, and Q. Xia, "A general formulation of linear power flow models: Basic theory and error analysis," *IEEE Trans. Power Syst.*, vol. 34, no. 2, pp. 1315–1324, 2019.

[14] M. Vrakopoulou, M. Katsampani, K. Margellos, J. Lygeros, and G. Andersson, "Probabilistic security-constrained ac optimal power flow," in *2013 IEEE Grenoble Conference*, 2013, pp. 1–6.

[15] Z. Fan, Z. Yang, and J. Yu, "Error bound restriction of linear power flow model," *IEEE Transactions on Power Systems*, vol. 37, no. 1, pp. 808–811, 2022.

[16] J. Long, W. Jiang, L. Jin, T. Zhang, H. Jiang, and T. Xu, "A combination of linear power flow models to reduce linearization error," in *2020 IEEE 3rd International Conference of Safe Production and Informatization (IICSPI)*, 2020, pp. 256–260.

[17] A. J. Wood, B. F. Wollenberg, and G. B. Sheblé, *Power generation, operation, and control*. John Wiley & Sons, 2013.

[18] B. Eldridge, R. O'Neill, and A. Castillo, "An improved method for the dcopf with losses," *IEEE Trans. Power Syst.*, vol. 33, no. 4, pp. 3779–3788, 2017.

[19] H. Sun, Q. Guo, B. Zhang, W. Wu, and B. Wang, "An adaptive zone-division-based automatic voltage control system with applications in china," *IEEE Trans. Power Syst.*, vol. 28, no. 2, pp. 1816–1828, 2012.

[20] T. Akbari and M. T. Bina, "Linear approximated formulation of ac optimal power flow using binary discretisation," *IET Gener. Transm. Distrib.*, vol. 10, no. 5, pp. 1117–1123, 2016.

[21] K. Dvijotham and D. K. Molzahn, "Error bounds on the dc power flow approximation: A convex relaxation approach," in *2016 IEEE 55th Conference on Decision and Control (CDC)*, 2016, pp. 2411–2418.

[22] Z. Yang, H. Zhong, A. Bose, T. Zheng, Q. Xia, and C. Kang, "A linearized opf model with reactive power and voltage magnitude: A pathway to improve the mw-only dc opf," *IEEE Trans. Power Syst.*, vol. 33, no. 2, pp. 1734–1745, 2017.

[23] Z. Li, J. Yu, and Q. H. Wu, "Approximate linear power flow using logarithmic transform of voltage magnitudes with reactive power and transmission loss consideration," *IEEE Trans. Power Syst.*, vol. 33, no. 4, pp. 4593–4603, 2018.

[24] Z. Fan, Z. Yang, J. Yu, K. Xie, and G. Yang, "Minimize linearization error of power flow model based on optimal selection of variable space," *IEEE Trans. Power Syst.*, vol. 36, no. 2, pp. 1130–1140, 2020.

[25] Y. Liu, N. Zhang, Y. Wang, J. Yang, and C. Kang, "Data-driven power flow linearization: A regression approach," *IEEE Trans. Smart Grid*, vol. 10, no. 3, pp. 2569–2580, 2019.

[26] X. Pan, T. Zhao, M. Chen, and S. Zhang, "Deepopf: A deep neural network approach for security-constrained dc optimal power flow," *IEEE Trans. Power Syst.*, vol. 36, no. 3, pp. 1725–1735, 2021.

[27] H. Zhong, Q. Xia, Y. Wang, and C. Kang, "Dynamic economic dispatch considering transmission losses using quadratically constrained quadratic program method," *IEEE Trans. Power Syst.*, vol. 28, no. 3, pp. 2232–2241, 2013.

[28] Y. Liu, B. Xu, A. Botterud, N. Zhang, and C. Kang, "Bounding regression errors in data-driven power grid steady-state models," *IEEE Trans. Power Syst.*, vol. 36, no. 2, pp. 1023–1033, 2020.

[29] J. Chen, W. Wu, and L. A. Roald, "Data-driven piecewise linearization for distribution three-phase stochastic power flow," *IEEE Trans. Smart Grid*, pp. 1–1, 2021.

[30] M. Yao, D. K. Molzahn, and J. L. Mathieu, "An optimal power-flow approach to improve power system voltage stability using demand response," *IEEE Trans. Control Netw. Syst.*, vol. 6, no. 3, pp. 1015–1025, 2019.

[31] S. Axler, *Linear algebra done right*. Springer, 2015, vol. 2.

[32] S. Yalçinbaş, M. Sezer, and H. H. Sorkun, "Legendre polynomial solutions of high-order linear fredholm integro-differential equations," *Appl. Math. Comput.*, vol. 210, no. 2, pp. 334–349, 2009.

[33] K. M. Anstreicher, "Semidefinite programming versus the reformulation-linearization technique for nonconvex quadratically constrained quadratic programming," *Journal of Global Optimization*, vol. 43, no. 2, pp. 471–484, 2009.

[34] (2022) 3000 load samples for paper "component analysis and accuracy improvement of linear power flow equation based on legendre polynomial expansion". [Online]. Available: https://doi.org/10.6084/m9.figshare.20299821.v1

Zhexin Fan (S'20) received the B.S. degree from Huazhong University of Science and Technology in 2016. He currently pursues the Ph.D. degree in electrical engineering at Chongqing University. His research interests focus on the linear power flow model optimization.

Zhifang Yang (S'13-M'18) received the Ph.D. degree in electrical engineering from Tsinghua University in 2018. He currently works as an assistant professor at Chongqing University. His research interests include power system optimization and electricity market.

Juan Yu (M'07-SM'15) received the Ph.D. degree in electrical engineering from Chongqing University in 2007. She currently works as a full professor at Chongqing University. Her research interests include static equivalent, optimal reactive power flow, and risk assessment in power systems.

Thomas Morstyn (S'14-M'16) received the Ph.D. degree in electrical engineering from the University of New South Wales, Sydney, NSW, Australia, in 2016. He currently works as a lecturer at the University of Edinburgh. His research interests include multiagent control and market design for the integration of distributed energy resources into power systems.